Numerical Simulations of Pulsed-Air Mixing Technology using Multiphase Computational Fluid Dynamics Methods

Rinaldo G. Galdamez, Stephen Wood, Seckin Gokaltun
Florida International University, Applied Research Center, Miami, Florida 33174

ABSTRACT

COMSOL Multiphysics and OpenFOAM Computational Fluid Dynamics (CFD) methods are used to create a computational model of a pulsed-air mixer. First, results are provided for a benchmark problem with a single bubble rising due to buoyancy with density and viscosity ratios of 10. The numerical results are verified using the bubble circularity and the terminal bubble velocity at different meshing levels which is captured within 10% accuracy compared with the benchmark simulation.

After the verification of the numerical methods, the flow characteristics created by a pulsed-air mixer in a 1/12-scale tank based on Hanford double-shell tank dimensions are simulated using the proposed CFD methods. This scaled experiment was carried out by Pacific Northwest National Laboratory (PNNL) in 1996. The peak fluid velocities produced by the pulsed-air mixing plate are compared against the PNNL experimental data at various locations away from the plate. The simulations show that the proposed methods can predict the performance of the pulsed-air system accurately and they can be used as computational tools for scaling up the design of future pulsed-air mixing implementations at Department of Energy (DOE) waste tanks.

INTRODUCTION

As a result of atomic weapons production, millions of gallons of radioactive waste were generated and stored in underground tanks at various U.S. Department of Energy (DOE) sites. DOE is currently in the process of transferring the waste from single-shell tanks to double-shell tanks. In order to decrease the probability of a plug occurring during the transfer process, several tank mixing techniques have been devised and evaluated at these sites. One of these techniques, pulsed-air mixing, consists of the injection of discrete pulses of air or inert gas by means of accumulator plates located at the bottom of the tank. These pulses generate large bubbles that rise due to buoyancy and create circulation in the surrounding fluid which contributes to mixing of the contents in the tank. Pulsed-air mixers are operated by controlling the pulsing frequency, pulse duration, type of accumulator plates and gas pressure. In comparison with other mixing techniques, the main advantages of the pulsed-air mixers are the low cost, durability, and easy maintenance and decontamination.

This technology is commercially available and its effectiveness has been demonstrated at Pacific Northwest National Laboratory (PNNL) and Oak Ridge National Laboratory (ORNL). Various scenarios and waste conditions can occur at DOE sites; hence, it is important to develop a computational model of a typical pulsed-air mixing application that can serve as a tool for site engineers to predict mixing performance and to optimize operational parameters.

In this paper, such a computational model was developed with COMSOL Multiphysics and OpenFOAM CFD solvers using the phase field and volume-of-fluid multiphase methods, respectively. In this study, simulations were performed for two cases. The first one was a benchmark case for a single bubble rising for which the results are quantitatively analyzed and compared to a reference solution using the bubble circularity and the bubble rise mean velocity. The second test case was for the pulsed air mixer technology. In order to save computational time, the simulations were carried out in a two dimensional domain where only one half of the scaled tank was modeled. The parameters for the simulation, in terms of plate dimensions, pressure values, injection time and other geometrical properties, were obtained from the PNNL technical report by Powell et al. [1]. It was found that the peak fluid velocities obtained from the simulation were within an average relative error of 19% compared to the experimental values available in such report.

MATERIALS AND METHODS

The Phase-Field Method

The phase field method (PFM) is an approach based on free-energy for the modeling of multiphase flow problems that was used in the COMSOL Multiphysics software. This method is based on a Cahn-Hilliard equation, for which two second order partial differential equations are decomposed and solved. The use of the Cahn-Hilliard equation ensures that the total energy of the system diminishes correctly. The tracking of the interface between the two fluids is governed by the so-called phase field variable φ [2], [3].

The free energy of a system of two immiscible fluids consists of mixing, bulk distortion and anchoring energy. This type of energy is modeled as a function of the phase field variable φ.

$$\int f_{tot} dV = \int \left(\frac{1}{2} \varepsilon^2 |\nabla \varphi|^2 + f(\varphi, T) \right) dV, \quad \text{(Eq.1)}$$

Where ε is a measure of the interfacial thickness, controlled by the grid refinement parameter; and f_{tot} is the total free energy density of the system.

The evolution of the phase field variables is described by the following equation:

$$\frac{\partial \varphi}{\partial t} + (\boldsymbol{u}.\nabla)\varphi = \nabla.\gamma\nabla\left(\frac{\partial f_{tot}}{\partial \varphi} - \nabla.\frac{\partial f_{tot}}{\partial \nabla \varphi} \right), \quad \text{(Eq.2)}$$

Where $\boldsymbol{u}$ is the convective field and γ is a mobility parameter that serves to control the relaxation time that minimizes the total free energy.

The free energy density of an isothermal mixture of two immiscible fluids is comprised of the sum of the mixing energy and elastic energy. The mixing energy assumes the following form:

$$f_{mix}(\varphi, \nabla\varphi) = \frac{1}{2}\lambda|\nabla\varphi|^2 + \frac{\lambda}{4\varepsilon^2}(\varphi^2 - 1)^2, \quad \text{(Eq.3)}$$

Where λ is the mixing energy density. These parameters, along with ε, are related to the surface tension σ by the following expression:

$$\sigma = \frac{2\sqrt{2}}{3}\frac{\lambda}{\varepsilon}, \quad \text{(Eq.4)}$$

The Cahn- Hilliard equation governing the phase field variable is

$$\frac{\partial \varphi}{\partial t} + \boldsymbol{u}.\nabla\varphi = \nabla.\gamma\nabla G, \quad \text{(Eq.5)}$$

Where G is the chemical potential defined by:

$$G = \lambda\left[-\nabla^2\varphi + \frac{\varphi(\varphi^2-1)}{\varepsilon^2}\right], \quad \text{(Eq.6)}$$

For the solution process, COMSOL Multiphysics breaks down Eq.5 in two partial differential equations:

$$\frac{\partial \varphi}{\partial t} + \boldsymbol{u}.\nabla\varphi = \nabla.\frac{\gamma\lambda}{\varepsilon^2}\nabla\psi, \quad \text{(Eq.7a)}$$

$$\psi = -\nabla.\varepsilon^2\nabla\varphi + (\varphi^2-1)\varphi, \quad \text{(Eq.7b)}$$

For which ψ is called the phase field help variable. For laminar two-phase flow, the transport of mass and momentum is governed by the incompressible Navier-Stokes equations including surface tension (Eq. 8a-b).

$$\rho\left(\frac{\partial \boldsymbol{u}}{\partial t} + \boldsymbol{u}.\nabla\boldsymbol{u}\right) = -\boldsymbol{\nabla}p + \nabla.\eta\left(\nabla\boldsymbol{u} + \boldsymbol{\nabla u^T}\right) + \rho\boldsymbol{g} + \boldsymbol{F_{st}} \quad \text{(Eq.8a)}$$

$$\nabla.\boldsymbol{u} = \boldsymbol{0} \quad \text{(Eq.8b)}$$

The Volume-of-Fluid Method

In addition to the COMSOL Multiphysics software, another multiphase CFD code called OpenFOAM was utilized for comparison purposes. The multiphase solver used in OpenFOAM is called InterFoam. This solver uses the Volume of Fluid Method (VOF) to compute multiphase flows [4], [5].

One momentum equation and one continuity equation are solved for both fluid phases. The physical properties of one fluid are calculated as weighted averages based on the volume fraction of the two fluids in one cell. The momentum equation takes the form:

$$\frac{\partial \rho}{\partial t} + \nabla.(\rho\boldsymbol{u}\boldsymbol{u}) - \nabla.\mu\nabla\boldsymbol{u} - \rho g - F_s = 0, \quad \text{(Eq.9a)}$$

$$\nabla . \boldsymbol{u} = 0, \quad \text{(Eq.9b)}$$

The volume of fluid in a cell is computed as $F_{vol} = V_{cell}$, where V_{cell} is the volume of a computational cell and is the fluid fraction in a cell. The values of in a cell should range between 1 and 0. If the cell is completely filled with fluid then the value equals to one and if it is filled with the other phase considered in the model then its value should be 0. At the interface, the value is between 0 and 1. The scalar function can be computed from a separate transport equation that takes the form:

$$\frac{\partial \gamma}{\partial t} + \nabla . (\gamma \boldsymbol{u}) = 0, \quad \text{(Eq.10)}$$

In OpenFOAM, the necessary compression of the surface is achieved by introducing an extra artificial compression term into the VOF equation given as:

$$\frac{\partial \gamma}{\partial t} + \nabla . (\gamma \boldsymbol{u}) + \nabla . (\gamma(1-\gamma)\boldsymbol{u_r}) = 0, \quad \text{(Eq.11)}$$

Where $\boldsymbol{u_r}$ is a velocity field suitable to compress the interface. This artificial term is active only in the interface region due to the term $\gamma(1-\gamma)$. The density at any point in the domain is calculated as a weighted averaged of the volume fraction of the two fluids as $\rho = \gamma\rho + (1-\gamma)\rho$. The surface tension F_s is computed as $F_s = \sigma\kappa(x)n$, where n is a unit vector normal to the interface that can be calculated by $n = \frac{\nabla \gamma}{|\nabla \gamma|}$.

Turbulence Modeling: Large Eddy Simulation (LES)

A turbulence model was also explored for the CFD simulation of the pulsed air mixer. Large eddy simulation (LES) is based on the computation of large energy-containing structures that are resolved on the computational grid, where smaller, more isotropic, subgrid structures are also modeled [6] [7]. This separation of scales is accomplished implicitly in the finite volume method with low-pass filtering of the Navier-Stokes Equations. Hence, starting from the incompressible Navier-Stokes equations:

$$\partial_t(\rho \mathbf{v}) + \nabla . (\rho \mathbf{v} \otimes \mathbf{v}) = -\nabla p + \nabla . \boldsymbol{S}, \quad \text{(Eq.12)}$$

$$\nabla . (\rho \mathbf{v}) = 0, \quad \text{(Eq.13)}$$

Where $\mathbf{v}$ is the velocity, p is the pressure, $\boldsymbol{S} = 2\mu\boldsymbol{D}$ is the viscous stress tensor, where the rate-of-strain tensor is expressed as $\boldsymbol{D} = \frac{1}{2}(\nabla v + \nabla v^T)$, and μ is the viscosity. The LES equations are theoretically derived from Eq.12 by applying low-pass filtering, using a pre-defined filter kernel function $G = G(\mathbf{x}, \Delta)$, such that:

$$\partial_t(\rho \bar{\mathbf{v}}) + \nabla . (\rho \bar{\mathbf{v}} \otimes \bar{\mathbf{v}}) = -\nabla \bar{p} + \nabla . (\bar{\boldsymbol{S}} - \boldsymbol{B}), \quad \text{(Eq.14)}$$

$$\nabla . (\rho \bar{\mathbf{v}}) = 0, \quad \text{(Eq.15)}$$

Where overbars denote filtered quantities and commutation errors are not taken into account. Eq.14 introduces one new term when compared to the unfiltered Eq.12: the unresolved transport term $\nabla \boldsymbol{B}$, where,

$$\boldsymbol{B} = \rho(\overline{\mathbf{v}\otimes\mathbf{v}} - \bar{\mathbf{v}}\otimes\bar{\mathbf{v}}), \quad \text{(Eq.16)}$$

is the subgrid stress tensor. Following B can be exactly decomposed as

$$\boldsymbol{B} = \rho\left(\overline{\bar{\mathbf{v}}\otimes\bar{\mathbf{v}}} - \bar{\bar{\mathbf{v}}}\otimes\bar{\bar{\mathbf{v}}} + \widetilde{\boldsymbol{B}}\right), \quad \text{(Eq.17)}$$

Where now only $\widetilde{\boldsymbol{B}}$ is modeled. For this paper, no subgrid modeling approach is applied. This type of modeling is named implicit LES or ILES.
Regarding the wall treatment, LES required near-wall mesh refinement compared to the rest of the free-stream flow mesh resolution in order to correctly and accurately solve for the energetic structures. Since this procedure is computationally expensive, a logarithmic law function is used along the wall which is implemented with an adjustment of the viscosity for the cells close to the wall.

Important dimensionless parameters

For the benchmark case of a single bubble dynamics under gravity, three fundamental non-dimensional numbers are used to describe the deformation of the bubble. These non-dimensional numbers are quite useful, since it allows for a specific test case to be located in the bubble deformation curve proposed by Clift et al [8]. Also, these non-dimensional numbers can serve as a common ground of comparison between CFD methods such as Phase Field method and Volume-of-Fluid Method. The Eötvös number (Eo), Morton number (M) and Reynolds number (Re) can be obtained through the Buckingham Pi Theorem [9].

The Eötvös number (Eo) and Morton number (M) are defined as follows:

$$E_o = \frac{\Delta\rho . g . d^2}{\sigma}, \qquad M = \frac{g{\mu_l}^4\Delta\rho}{{\rho_l}^2\sigma^3} \quad and \quad Re = \frac{\rho_1 U_g L}{\mu_1}, \quad \text{(Eq.18)}$$

Where $\Delta\rho$ is the difference in density of the two phases, g is the gravitational acceleration, L is the characteristic length, σ is the surface tension, μ_l is the viscosity of the surrounding fluid, ρ_l is the density of the surrounding fluid, ρ_1 is the density of the bubble, μ_1 is the viscosity of the bubble, and U_g is the velocity of the bubble given by $\sqrt{2gr}$ where r is the initial radius of the bubble.

BENCHMARK COMPUTATIONS

COMSOL and OpenFOAM simulations were performed for a single bubble benchmark case presented by Hysing et al. [10]. In this benchmark case, several academic codes (TP2D, MooNMD and FreeLIFE) were used to simulate a well-defined problem and the results were compared against commercially available codes such as CFX, Fluent and COMSOL Multiphysics. The non-dimensional flow parameters for the benchmark test case are given in the table below.

Table I. Parameters for the Validation Case

ρ1	ρ2	μ1	μ2	g	σ	Re	Eo	M	ρ1/ρ2	μ1/μ2
1000	100	10	1	0.98	24.5	35	10	0.0006	10	10

The schematic of the non-dimensional geometry configuration is shown Fig.1 below.

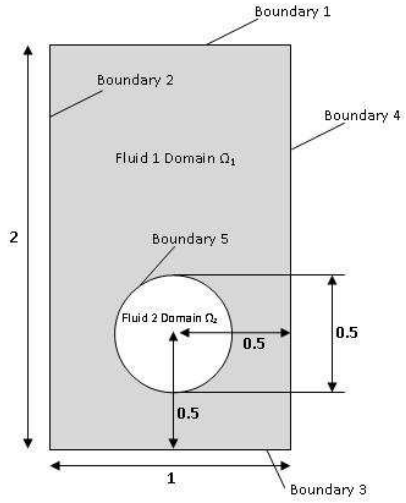

Fig. 1. Domain configuration and boundaries for the benchmark test case.

Domains Ω_1 and Ω_2 are the domains for fluid 1 and fluid 2, respectively. Boundaries 1 and 3 are set to wall type boundary with no slip condition. Boundaries 2 and 4 are set as symmetry (slip) boundary type. Boundary 5 is the fluid interface. The initial diameter d_i of the bubble is 0.5.

In order to determine level of discretization error, a mesh convergence study is performed with both COMSOL Multiphysics and OpenFOAM. The quantitative analysis of the results is evaluated with two quantities: the bubble circularity and the bubble rise mean velocity [10].

The centroid of the bubble is defined as:

$$\boldsymbol{X}_c = (x_c, y_c) = \frac{\int_{\Omega_2} \boldsymbol{x}\, dx}{\int_{\Omega_2} 1\, dx}, \quad \text{(Eq.19)}$$

For which Ω_2 is the domain occupied by the bubble.

The circularity is given by the following expression:

$$c = \frac{P_a}{P_b} = \frac{perimeter\ of\ circle\ with\ equivalent\ area}{perimeter\ of\ bubble} = \frac{\pi d_{eq}}{P_b}, \quad \text{(Eq.20)}$$

The mean rising velocity for the bubble is given by

$$\boldsymbol{U}_c = \frac{\int_{\Omega_2} \boldsymbol{u}\, dx}{\int_{\Omega_2} 1\, dx}, \qquad \text{(Eq.21)}$$

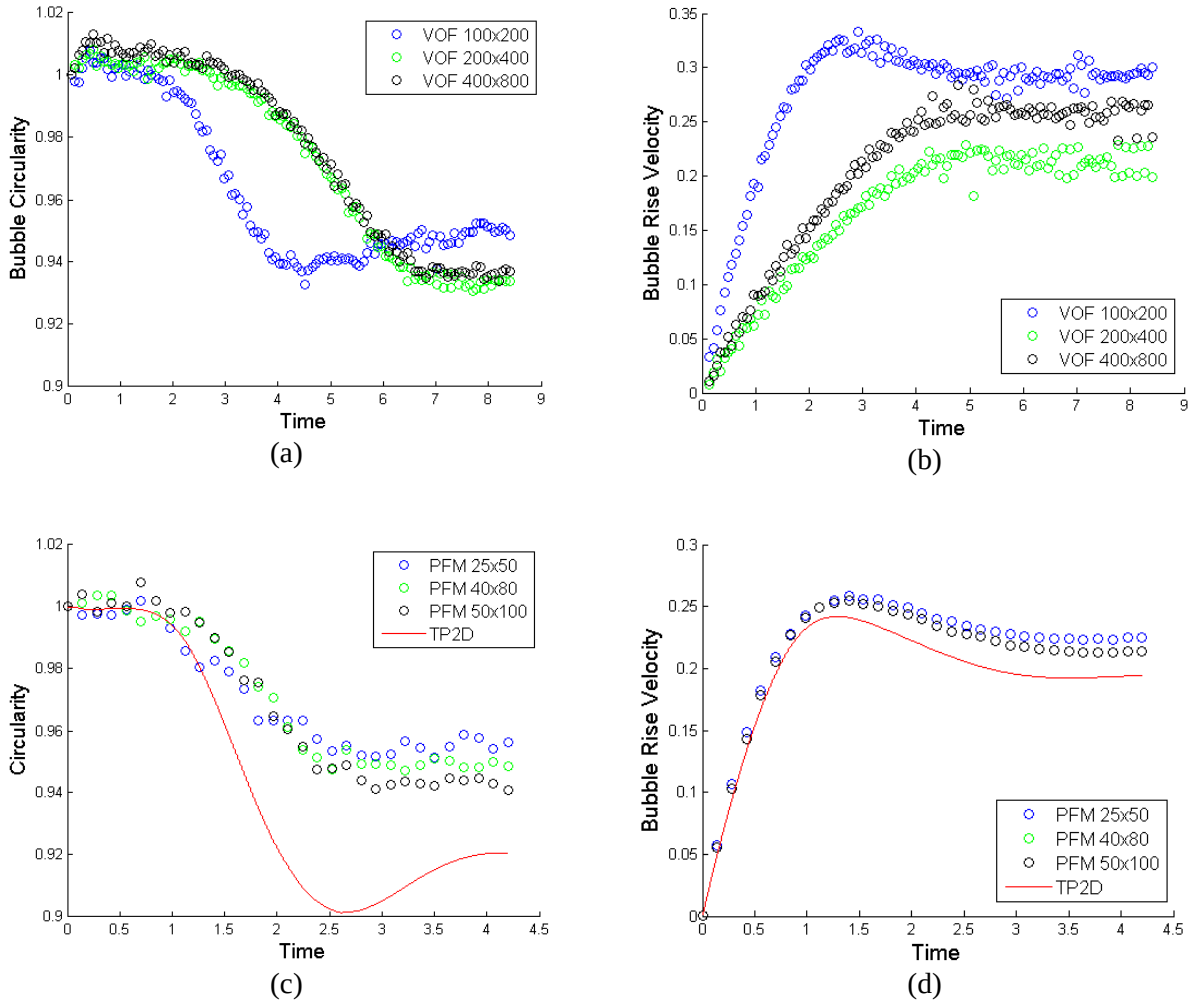

Fig.2 : Circularity and bubble rise mean velocity using VOF and PFM. The time in this plot is non-dimensionalized by $T = {}^{t}/_{t_{ref}}$ where $t_{ref} = \sqrt{{}^{d_i}/_{g}}$

The shape of the bubble can be analyzed qualitatively by comparing the deformed interface with the reference solution and the bubble shape diagram given by Clift et al [8]. Given the value of the Eo, M and Re numbers, the expected bubble shape that corresponds to the flow conditions of the test case can be located in such diagram that could be one of the following: spherical, ellipsoidal, wobbling, dimpled ellipsoidal cap, skirted or spherical cap. In the case analyzed for this paper, the shape would correspond to an ellipsoidal shaped deformation.

Fig.2 shows the quantitative analysis performed for this test case, where the influence of the mesh size can be observed in regards to the convergence of the results compared to the available published solution.

The circularity and the bubble rise mean velocity were analyzed using both the PFM and VOF methods (Fig. 2a and 2c). Fig. 2d presents the rise velocity as a function of time. The bubble velocity reaches a constant value after about T=2.5. These results agree within 10% error and any discrepancy observed in both the circularity and velocity plots may be the result of the difference between PFM and the level set method adopted in the reference solution [10], [11].

In regards to the results presented for the VOF method, it can be observed that the curve tendency is similar to the one observed with PFM in Fig. 2a and Fig. 2c. It is interesting to point out that the bubble takes more time to deform in the simulation with OpenFOAM using the VOF method. In non-dimensional time, for PFM and TP2D, the bubble has reached its terminal shape at around T=4.5, whereas at this time, VOF is still showing the highest deformation point in the circularity plot and has not reached the terminal shape.

Similar comments can be made for the velocity plot (Fig. 2b) where the terminal velocity is reached after T=4. The value for the terminal velocity for the VOF mesh of 200x400 is close to the value given by the reference solution; however, the highest mesh resolution of 400x800 shows a higher value for the bubble mean rise velocity.

The differences observed between the results achieved with OpenFOAM and COMSOL Multiphysics could be due to the variance of the numerical methods used in each these CFD solvers. OpenFOAM uses finite volume whereas COMSOL is a finite element based software package.

RESULTS

Parameters

The simulations are performed on a two dimensional domain, for which Fig. 3e shows the different values of the dimensions considered. The $h_{standoff}$ distance represents the vertical distance that separates both accumulator plates. The R_{tank} is the radius of the tank, since only one half of the PNNL 1/12 scaled experimental test tank is simulated. The value of h_{vel} corresponds to the location at which the velocity is measured for the different probe points in the experiment and simulation. The distance H_{tank} represents the height level of the water inside the tank. The blue dotted line represents the tube connected to the accumulator plates and through which the high pressure air is injected into the tank.

PNNL studied the velocities created by the expanding bubble around the accumulator plate pulsed-air mixing technology by attaching an anemometer to a rail on top of the tank; this anemometer was placed at 8, 11, 15 and 19 cm respectively from the plate centerline (middle of blue dotted line in Fig. 3e).

During the experimental testing, PNNL used accumulator plates of several diameters (6.1 cm, 14.2 cm, 23.9 cm, and 36.6 cm) at different values of injection pressure (20 psi, 40 psi, 60 psi, 80 psi, 100 psi) and different gas pipe diameters.

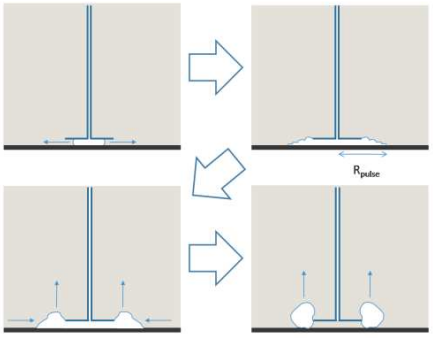

(a) Sketch of bubble growth during pulsed-air mixing

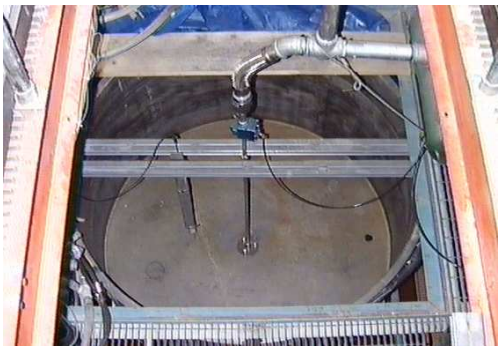

(b) Pulsed-air mixing experimental setup at PNNL

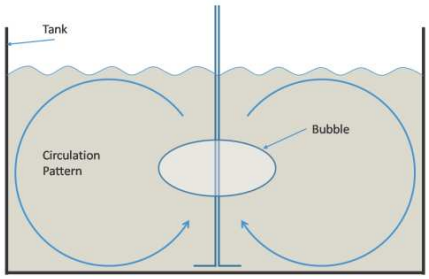

(c) Sketch showing mixed pattern induced by rising bubble

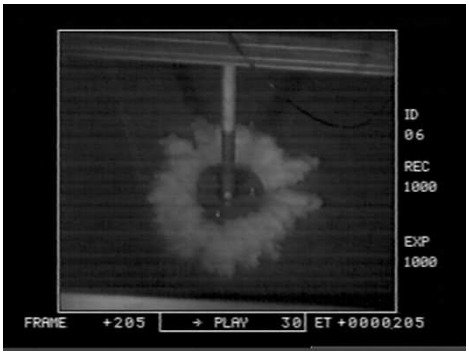

(d) High speed photo showing bubble growth in accumulator plate

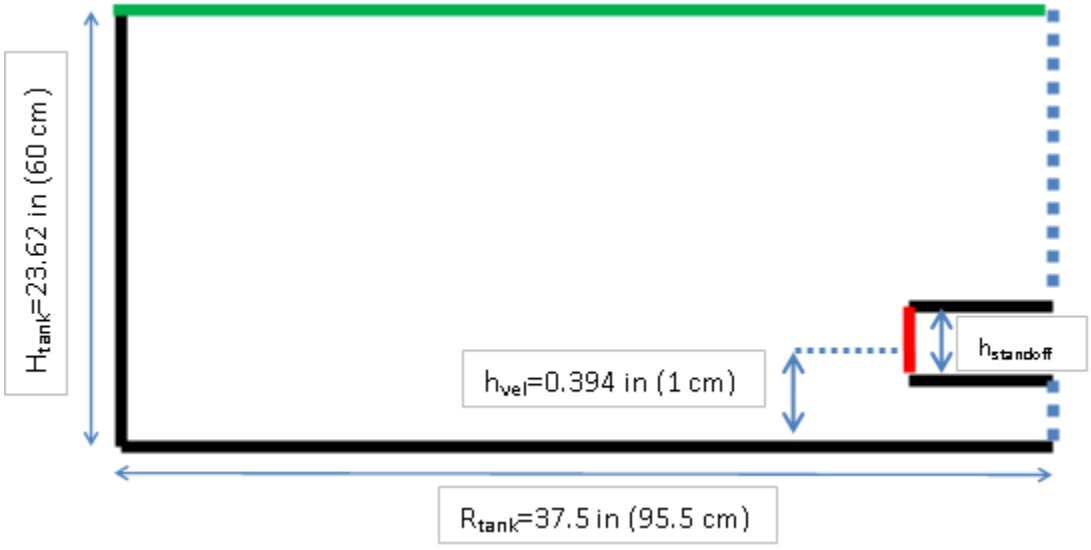

(e) Schematics for the simulations performed in COMSOL and OpenFOAM

Fig..3.Description of the computational and experimental set-up for the testing of the pulsed-air mixing technology.

For this paper, one case is simulated for which the parameters of pressure, standoff distance and the plate diameter are given in Table II.

According to the experimental data provided by PNNL, the fluid temperature varied between 13.2 ºC to 13.4º C, hence the viscosities, densities and surface tension for air and water, which were the two fluids considered, were set accordingly.

Moreover, during the experimental setup, the pulse injection time was set to 0.4 s, from the opening of the valve to the moment where the pulse is cut off.

Table II: Parameters for the Simulations for the Pulsed-Air Mixing

Case #	Pressure (psig)	Standoff distance (cm)	Plate Diameter (cm)	Gas pipe
1	20	0.635	6.1	1/8 S40

Mesh Convergence Study

In order to build the proper structured mesh for the turbulent simulation performed in OpenFOAM using LES, a mesh convergence study was completed for which the results are presented below in Fig. 4. This study corresponds to case 1 with an injection time of 0.4 seconds. The water velocities at four sensor locations were plotted along with the phase fraction recorded at each sensor location. The coarsest mesh contained 27,540 cells, the medium resolution mesh contained 110,160 cells, and the finest mesh contained 440,640 cells. As the resolution of the simulations increases, it becomes easier to discern the nearly linear increase of the water velocity at each sensor location in advance of the arrival of the air-water interface. The low resolution simulation results reveal significant numeric noise in the captured velocities as the air-water interface nears each sensor. The larger cells in the low resolution simulation cause the interface to be diffused and consequently phase fraction values well below 1 are reported. The air-water interface is defined as $\alpha = 0.5$ for all simulations.

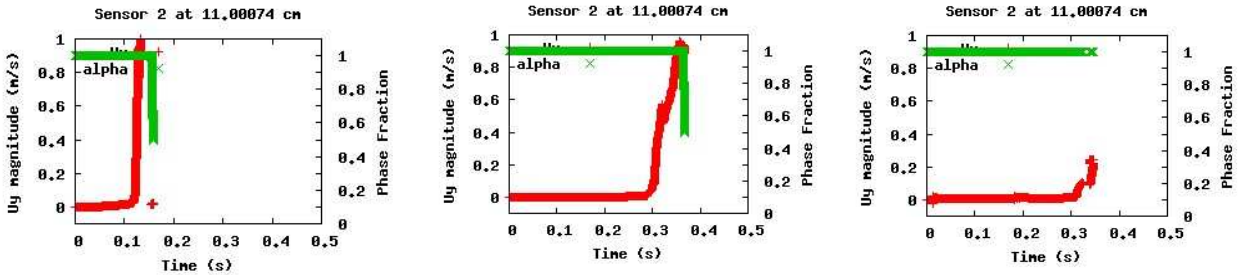

Low resolution Medium Resolution High Resolution

Fig. 4: Convergence study results for the pulsed-air mixing simulation case.

Pulsed-air mixing simulations

The simulations for the pulsed-air mixing technology were performed using the PFM and LES methods. First, a laminar flow simulation was performed using PFM in COMSOL Multiphysics.

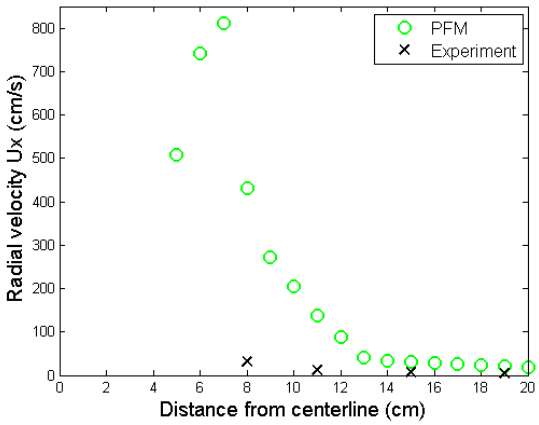

(a) Radial Velocity vs. Distance from centerline for PFM

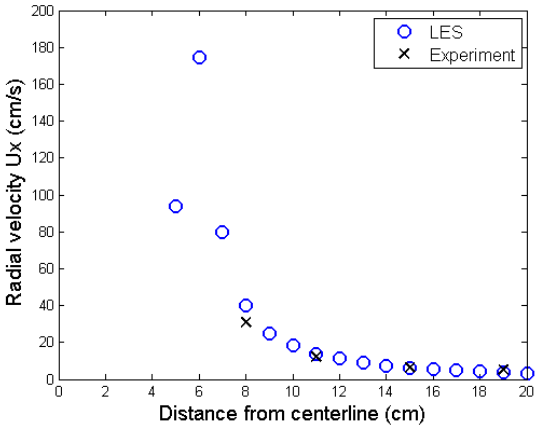

(b) Radial Velocity vs. Distance from centerline for LES

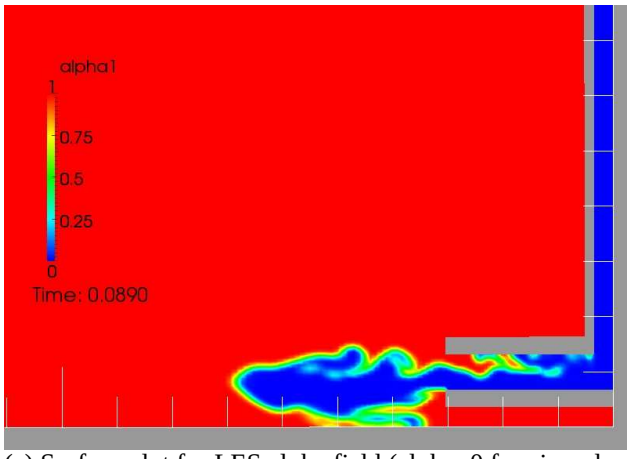

(c) Surface plot for LES alpha field (alpha=0 for air and alpha=1 for water)

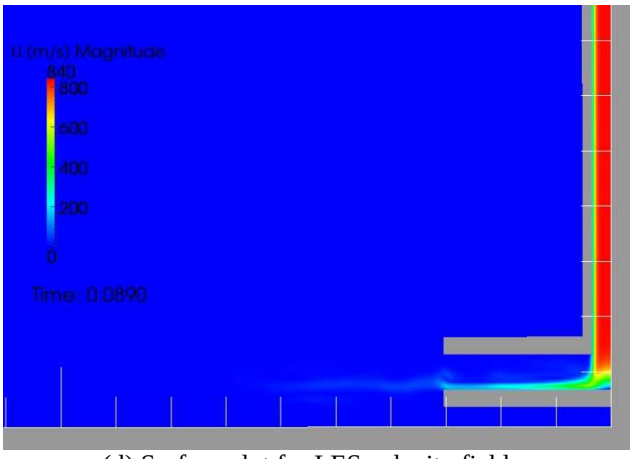

(d) Surface plot for LES velocity field

Fig. 5: Simulation results for Pulsed-air Mixing.

The results for this model are shown in Fig.5a, where it can be observed that the velocities calculated by PFM were very different from the ones gathered during the experiment. The average relative error for this simulation is 755.82%, which is not acceptable in any type of CFD simulation. However, several conclusions were drawn from this simulation which served to accurately simulate Case 1 with a turbulence model. Since the velocities given by PFM were not reasonable, it was inferred that PFM alone assuming an incompressible laminar flow inside the pipe and beyond the accumulator plate was not sufficient for the given conditions of the model.

As previously stated, the effect of temperature was already taken into account in order to cross out any source of discrepancy in regards to the fluid parameters that might be influencing the laminar flow simulation.

Hence, a quick calculation on the flow velocity inside the pipe using Bernoulli's equation was performed and yielded that the velocity of water would be in the order of 16 m/s and the velocity of air would be in the order of 462 m/s. Taking into account the gas pipe diameter, the Reynolds number (Re) was calculated accordingly, which resulted in $Re_{air} = 2.94 \times 10^5$ and $Re_{water} = 1.23 \times 10^5$.

The calculation of the previous parameters made it clear that the flow inside the pipe and therefore between and beyond the accumulator plates will also be highly turbulent. It was decided to run this simulation with the LES turbulence model available in OpenFOAM.

The results for this turbulence simulation are shown in Fig. 5b where a clear difference can be observed in comparison with the laminar flow simulation from Fig. 5b. The results agree with the experimental data with an average relative error of 19%. For both plots in Fig.5, more probe points were added in order to obtain a better velocity profile as a function of the distance from the centerline.

Moreover, Fig.5c and 5d show the surface plots that are obtained for the alpha field in OpenFOAM. As specified, the α field is equal to 0 for air and 1 for water. In Fig.5c, The turbulent flow structures can be observed inside and beyond the accumulator plates. In Fig.5d, the surface plot shows a considerably high value for the velocity field inside the gas pipe with a maximum of 840 m/s.

From the observed plots, it is clear that the CFD simulation of the pulsed-air mixing technology requires the implementation of an incompressible flow turbulence model in order to yield good results. The discrepancies between LES and the experimental data could be due to initial values assumed in the flow field for the LES model in OpenFOAM, which could be optimized to a proper value in order to increase accuracy.

DISCUSSION AND CONCLUSION

The CFD capabilities of COMSOL Multiphysics and OpenFOAM were implemented for the simulation of the single bubble benchmark study and the pulsed-air mixing technology. For the first simulation, it was shown that both numerical solvers are able to accurately model the single bubble validation study.

The PNNL experimental setup for the pulsed-air mixing technology was modeled in both numerical solvers in a two-dimensional space and half of the fluid domain in order to efficiently use the available computational resources. By observing the results of the simulation undertaken with PFM in COMSOL Multiphysics, it can be concluded that a turbulence model is essential to the accurate modeling of this type of mixing technology. The results provided by LES are in agreement with the experimental data provided by PNNL within a low and reasonable margin of

error. Hence, it can also be concluded that simulating this application in a two-dimensional space does not hinder the ability of achieving good results with the numerical solvers. This is of primary importance for CFD modelers involved in this type of application since simulations in a 2D space are much less computationally expensive.
For future work, the turbulence capabilities of COMSOL Multiphysics will be investigated and implemented using the available $k-\epsilon$ and $k-\omega$ turbulence models [12]. More importantly, the effects of air pressure and plate diameter presented in the PNNL report [1] will also be simulated with both OpenFOAM and COMSOL Multiphysics.

REFERENCES

[1] M R Powell and C R Hymas, "Retrieval Process Development and Enhancements FY96 Pulsed-Air Mixer Testing and Deployment Study," Pacific Northwest National Laboratory, Richland, WA, PNNL-1120, UC-721, 1996.

[2] COMSOL AB, *COMSOL User Guide- Chemical Engineering Module*. Trondheit, Sweden, 2008.

[3] Pengtao Yue, Chungfeng Zhou, James J Feng, Carl F Olliver-Gooch, and Howard H Hu, "Phase-Field simulations of interfacial dynamics in viscoelastic fluids using finite elements with adaptive meshing," *Journal of Computational Physics*, vol. 219, no. 1, pp. 47-67, November 2006.

[4] O Ubbink and R I Issa, "A Method for Capturing Sharp Fluid Interfaces on Arbitrary Meshes," *Journal of Computational Physics*, vol. 153, pp. 26-50, 1999.

[5] Henrik Rusche, "Computational Fluid Dynamics of Dispersed Two-Phase Flows at High Phase Fractions," University of London, Imperial College, London, Ph.D. Thesis 2002.

[6] Rickard E Bensow and Goran Bark, "Implicit LES Predictions of the Cavitating Flow on a Propeller," *Journal of Fluids Engineering*, vol. 132, April 2010.

[7] Rickard E Bensow and Goran Bark, "Simulating Cavitating Flows with LES in OpenFOAM," in *V European Conference on Computational Fluid Dynamics* , Lisbon, Portugal , 2010.

[8] R Clift, J R Grace, and M E Weber, *Bubbles, Drops and Particles*. New York, USA: Academic Press, 1978.

[9] Garrett Birkhoff, *Hydrodinamics: A study in Logic, Fact and Similitude*. Princeton: Princeton University Press, 1960.

[10] S Hysing et al., "Quantitative benchmark computation of two-dimensional bubble dynamics," *International Journal for Numerical Method in Fluids*, vol. 60, pp. 1259-1288, 2008.

[11] Elin Olsson and Gunilla Kreiss, "A Conservative level set method for two phase flow," *Journal of Computational Physics*, pp. 225-246, 2005.

[12] David C Wilcox, *Turbulence Modeling for CFD*.: DCW Industries, 2006.